Equivalent-Circuit Generation from Finite Element Solution Using Proper Orthogonal Decomposition

Toshihito Shimotani, Yuki Sato and Hajime Igarashi, *Member IEEE*

Graduate School of Information Science and Technology, Hokkaido University, Sapporo, 060-0184, Japan
simotani@em-si.eng.hokudai.ac.jp

This paper presents generation of equivalent circuits from finite element (FE) model of electromagnetic devices using proper orthogonal decomposition (POD). This method effectively computes the frequency response of the reduced FE model constructed by POD-based model order reduction. Then the circuit parameters are determined so as to minimize the error between the frequency responses of the reduced FE model and equivalent circuit. The frequency characteristics of an inductor and induction heating machine evaluated by the equivalent circuit are shown to be in good agreement with those computed from the original FE model.

***Index Terms*— Equivalent circuit, finite element method, induction heating, model order reduction.**

I. Introduction

FINITE element method (FEM) has been widely performed for design of electric machines and devices. However, due to its long computational time, equivalent circuits are frequently used rather than FEM for design of driving and control circuits. When deriving equivalent circuits of electric devices such as inductors and reactors, for example, the circuit parameters are determined from resistance and reactance computed by FEM [1,2]. It would be, however, difficult to accurately express its frequency characteristics over wide range using this conventional method.

Recently the equivalent circuit of ladder configuration has been directly derived from the analytical expression of eddy currents in electrical steel sheets [3]. This method would be valid for fields in simple geometry which can be expressed in a closed form. Now, a question arises; is it possible to generate equivalent circuits not only from closed-form solutions but also from FE solutions? Such equivalent circuits could be generated if the frequency characteristics are available. However, for large FE models, we need heavy computations to obtain the frequency characteristics over sufficiently wide range.

In this paper, we propose eqivalent-circuit generation from FE solutions using model order reduction (MOR) [4,5] based on proper orthogonal decomposition (POD). In this method, fields are expressed as a linear combination of small number of basis vectors obtained from the field snapshots [6-9]. In the proposed method, the computational time necessary for FE analysis is reduced by POD-based MOR. This method allows us to effectively compute the frequency responses for circuit generation. The circuit parameters are then determined so as to minimize the error between the frequency responses of the reduced FE model and equivalent circuit.

In this study, we apply the proposed method to a simplified three dimensional inductor model and compare the accuracy and computational time of the resultant equivalent circuit with those of the original FE model. Moreover, we apply it to the three-dimensional model of an induction heating (IH) machine to obtain the frequency-dependent power factor and joule loss.

Manuscript received July 6, 2015. Corresponding author: Toshihito Shimotani (e-mail: simotani@em-si.eng.hokudai.ac.jp).
Digital Object Identifier (inserted by IEEE).

II. Numerical Method

A. Proper orthogonal decomposition

Let us consider quasi-static electromagnetic fields described by FE equations in frequency domain given by

$$\sum_i a_i \int_\Omega \left(\mathrm{rot}\boldsymbol{N}_j \cdot \nu \mathrm{rot}\boldsymbol{N}_i + j\omega\kappa \boldsymbol{N}_i \cdot \boldsymbol{N}_j\right)\mathrm{d}V + \sum_k \varphi_k \int_\Omega j\omega\kappa \boldsymbol{N}_j \cdot \mathrm{grad}N_k \mathrm{d}V = \int_\Omega \boldsymbol{N}_j \cdot \boldsymbol{J}\mathrm{d}V \tag{1}$$

$$\sum_i a_i \int_\Omega j\omega\kappa \boldsymbol{N}_i \cdot \mathrm{grad}N_u \mathrm{d}V + \sum_k \varphi_k \int_\Omega j\omega\kappa \mathrm{grad}N_k \cdot \mathrm{grad}N_u \mathrm{d}V = 0 \tag{2}$$

where a_i, $\boldsymbol{N}_j$, ν, κ, φ_k and $\boldsymbol{J}$ denote magnetomotive force along an edge i, edge basis function, magnetic reluctivity, electric conductivity, scalar potential and current density. The electromagnetic field is assumed to be coupled with a circuit governed by

$$V = Ri + L\frac{\mathrm{d}i}{\mathrm{d}t} + \frac{\mathrm{d}\Phi}{\mathrm{d}t} \tag{3}$$

where V, R, L, i and Φ denote input voltage, external resistance and inductance, current and the magnetic flux computed from a_i. Eqs. (1), (2) and (3) are expressed in a matrix form as

$$\mathrm{K}(\mathrm{j}\omega)\boldsymbol{x} = \boldsymbol{b}(\mathrm{j}\omega) \tag{4}$$

where $\mathrm{K}\in R^{n\times n}$, $\boldsymbol{x}\in R^n$, $\boldsymbol{b}\in R^n$ are FE matrix, unknown and source vectors, respectively. We solve (4) at s different

frequencies to construct the data matrix X which is composed of the snapshotted fields as follows:

$$\mathrm{X} = \left[\boldsymbol{x}_1(\omega_1) \quad \boldsymbol{x}_2(\omega_2) \quad \cdots \quad \boldsymbol{x}_s(\omega_s)\right] \tag{5}$$

The singular value decomposition applied to X results in

$$\mathrm{X} = \mathrm{W}\Sigma\mathrm{V}^{\mathrm{t}} = \sigma_1\boldsymbol{w}_1\boldsymbol{v}_1^{\mathrm{t}} + \sigma_2\boldsymbol{w}_2\boldsymbol{v}_2^{\mathrm{t}} + \cdots + \sigma_s\boldsymbol{w}_s\boldsymbol{v}_s^{\mathrm{t}} \tag{6}$$

where σ_i is i-th singular value of X and $\boldsymbol{w}_i$, $\boldsymbol{v}_i$ are the eigenvectors of XX^{t} and $\mathrm{X}^{\mathrm{t}}\mathrm{X}$, respectively. The unknown $\boldsymbol{x}$ is now expressed as a linear combination of $\boldsymbol{w}_i$, that is, $\boldsymbol{x}=\mathrm{W}\boldsymbol{y}$ where $\boldsymbol{y}\in R^s$. Thus (4) becomes

$$\mathrm{W}^{\mathrm{t}}\mathrm{K}(\mathrm{j}\omega)\mathrm{W}\boldsymbol{y} = \mathrm{W}^{\mathrm{t}}\boldsymbol{b}(\mathrm{j}\omega) \tag{7}$$

The snapshot number s is set much smaller than n so that one solves (7) much faster than (4) to obtain the frequency characteristics.

B. Equivalent-circuit generation

We derive the equivalent circuit from the frequency response obtained by solving (7). We employ here Foster- and Cauer-form networks shown in Fig. 1 [10]. In Foster realization, admittance $Y(\mathrm{j}\omega)$ is expressed by

$$Y(\mathrm{j}\omega) \approx \sum_{k=1}^{q} \frac{1}{R_k + \mathrm{j}\omega L_k} \tag{8}$$

where R_k, L_k and q denote resistance, inductance and number of the stage of the ladder circuit, respectively. On the other hand, in Cauer realization, impedance $Z(\mathrm{j}\omega)$ is expressed in a form of continued fraction as

$$Z(\mathrm{j}\omega) \approx \mathrm{j}\omega L_1 + \cfrac{1}{R_1 + \cfrac{1}{\mathrm{j}\omega L_2 + 1/(R_2 + \cdots)}} \tag{9}$$

To determine the circuit parameters $R_1,\cdots, R_q$ and $L_1,\cdots, L_q$, in (8) and (9), we solve the optimization problem defined by

$$f(\boldsymbol{R},\boldsymbol{L}) = \sqrt{\sum_{i}^{M}\left|G^{\mathrm{FEM}}(\mathrm{j}\omega_i) - G(\mathrm{j}\omega_i,\boldsymbol{R},\boldsymbol{L})\right|^2} \to \min. \tag{10}$$

$$\text{sub. to } R_k, L_k \geq 0$$

where $\boldsymbol{R} = [R_1, R_2, \cdots, R_q]$, $\boldsymbol{L} = [L_1, L_2, \cdots, L_q]$, $G^{\mathrm{FEM}}(\mathrm{j}\omega_i)$, $G(\mathrm{j}\omega_i,\boldsymbol{R},\boldsymbol{L})$ represent either Y or Z obtained by solving (7) and from the derived equivalent circuit and M is the number of sampling points for circuit identification, where $M>s$. The optimization problem (10) is solved here using the real coded genetic algorithm (RGA). The process of the proposed method is illustrated in Fig. 2.

III. Numerical Results

To test performance, the proposed method is applied to models of an inductor and IH machine.

A. Simplified inductor model

Let us consider an inductor connected to the simple circuit shown in Fig. 3. The model parameters are summarized in Table I. The magnetic core is assumed to be conductive although eddy currents in the coil windings are neglected.

Dependence of the relative error, $e=\|x^{\mathrm{FEM}}-x^{\mathrm{reduced}}\|/\|x^{\mathrm{FEM}}\|$, of the reduced model on s is shown in Fig.4. It can be seen in Fig.4 that the error is improved little even if when s is increased more than 6. For this reason, we take 6 snapshots with equal frequency intervals for $1 \leq f \leq 10^3$ Hz. Then, we solve (7) at 11 frequency points, f = 1, 100, 200, … , 10^3 Hz, to obtain the frequency characteristic of the inductor. That is, s=6, M=11.

The frequency characteristics of the current obtained from the conventional FEM and the proposed method for different number of ladder stages q are shown in Fig.5. The proposed

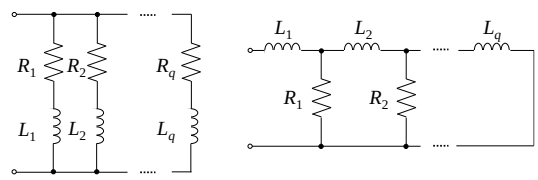

(a) Forster circuit (b) Cauer circuit

Fig. 1. Equivalent circuits

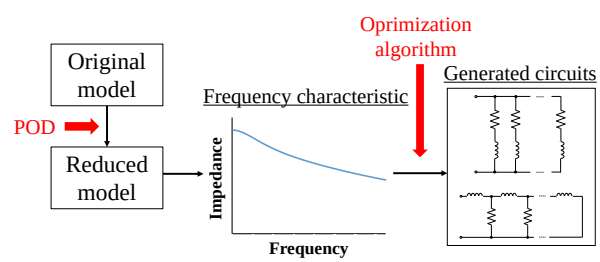

Fig. 2. Processes of prosed method

TABLE I
Analysis Condition

Electrical conductivity κ [S/m]	5.0×10^6
Relative permeability μ_r	10
External resistance R [Ω] / inductance L[H]	1.0×10^{-5} / 1.0×10^{-15}
Amplitude of the input voltage v [V]	1.0
Max frequency f_{max} [Hz]	1000
Number of the unknowns	370042

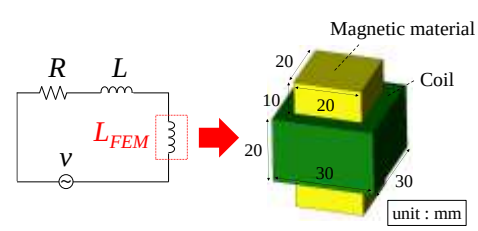

Fig. 3. Inductor model

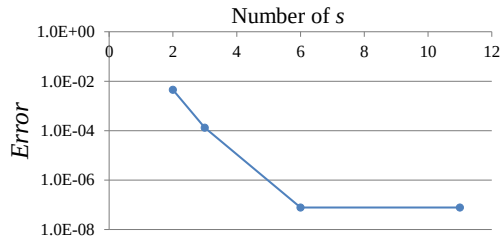

Fig. 4. Error study of the reduced model.

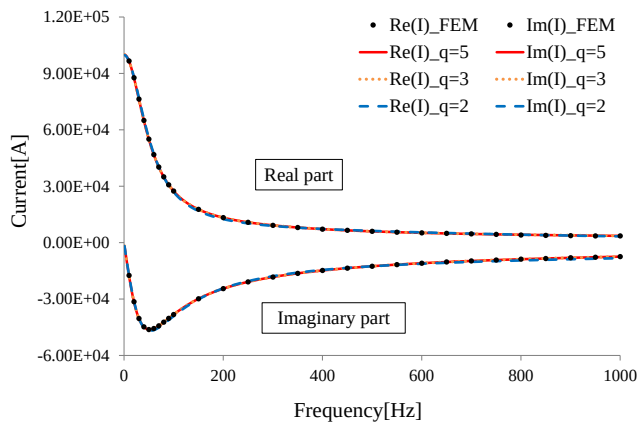

(a) Foster

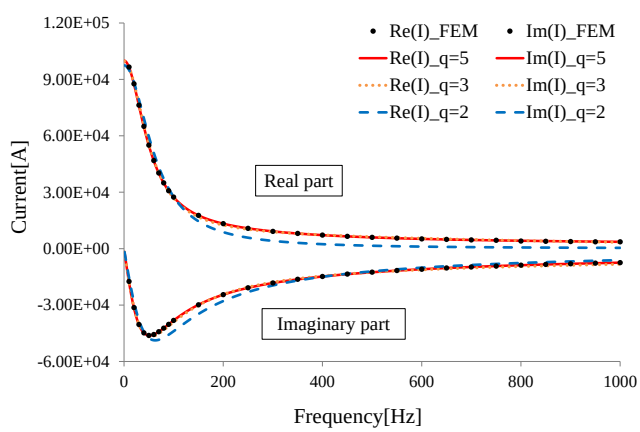

(b) Cauer

Fig. 5. Frequency characteristics of current

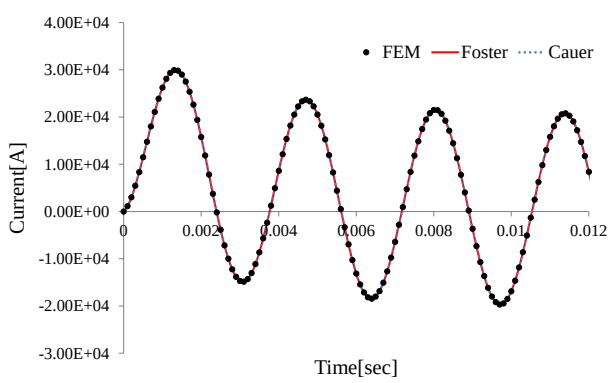

Fig. 6. Transient currents (300Hz, q=5)

method is found to be quite accurate even when q=3. The values of R, L for q=5 are summarized in Table II. Note that there is no uniqueness in these results. The ratio of computational time of the proposed method to that of conventional FEM depends on the number of points for frequency sweep. Computational times of the conventional FEM and the proposed method are summarized in Table III. It is also possible to perform transient analysis using the resultant equivalent circuit. The results are shown in Fig. 6, where we again find good correspondence among the results. Computational accuracy of the proposed method improves with s and M. The lower error bound estimated *a posteriori* is about 10^{-2} %.

TABLE II
Circuit parameters

Foster circuit					
q	R_1[Ω]	R_2[Ω]	R_3[Ω]	R_4[Ω]	R_5[Ω]
5	1.18×10^{-5}	4.91×10^{-4}	1.73×10^{-4}	5.59×10^{-4}	1.81×10^{-4}
3	3.35×10^{-4}	1.10×10^{-5}	1.55×10^{-4}	----	----
2	1.48×10^{-4}	1.08×10^{-5}	----	----	----
q	L_1[H]	L_2[H]	L_3[H]	L_4[H]	L_5[H]
5	3.68×10^{-8}	1.44×10^{-8}	8.74×10^{-8}	9.10×10^{-8}	6.73×10^{-7}
3	1.74×10^{-8}	3.48×10^{-8}	6.98×10^{-8}	----	----
2	2.56×10^{-8}	3.25×10^{-8}	----	----	----
Cauer circuit					
q	R_1[Ω]	R_2[Ω]	R_3[Ω]	R_4[Ω]	----
5	1.21×10^{-4}	2.43×10^{-5}	2.09×10^{-5}	3.64×10^{-4}	----
3	4.81×10^{-5}	1.27×10^{-5}	----	----	----
2	1.03×10^{-5}	----	----	----	----
q	L_1[H]	L_2[H]	L_3[H]	L_4[H]	L_5[H]
5	9.68×10^{-9}	1.54×10^{-8}	2.34×10^{-8}	3.68×10^{-7}	3.84×10^{4}
3	1.43×10^{-8}	2.23×10^{-8}	4.77×10^{-3}	----	----
2	2.60×10^{-8}	8.37×10^{-4}	----	----	----

TABLE III
Elapsed times for computations at 100 different frequencies

	M	Computational time [min]*
Conventional FEM	---	120
Proposed method	21	21.0
	16	16.4
	11	11.8

*Xeon X5660(2.8GHz) is used.

B. *Induction heating machine*

We next consider an IH machine model shown in Fig. 7, where a conducting sheet is heated up by Joule losses caused by eddy currents. The number of the unknowns in the original FE model are 741264. The AC currents flowing through the coil windings generate time variations in the magnetic flux, and eddy currents in the sheet. For the effective control of the IH machine, power factor which is the ratio of active power to reactive one is required to be as high as possible. Moreover, evaluation of the Joule loss is of importance for on-line control of the sheet temperature.

The power factor η and Joule loss P are computed by the conventional FEM as well as the equivalent circuit generated by the proposed method. They are computed from

$$P^{FEM} = \sum_{n_e} \int_{\Omega} \sigma \left| \boldsymbol{E} \right|^2 \mathrm{d}v \tag{12}$$

$$P^{Circuit} = \frac{V\dot{I}^*}{2} \tag{13}$$

where P^{FEM}, P^{Circit}, n_e, $\boldsymbol{E}$, V and $\dot{I}^*$ denote Joule losses computed from FE analysis and equivalent circuits, number of FEs and electric field, voltage and complex conjugate of current. The conditions of the snapshots and sampling points to generate the equivalent circuits are the same as those mentioned in III-A.

The frequency characteristics of η and P computed from the FEM and equivalent circuits are shown in Figs. 8 and 9 where V=1kV and resultant circuit parameters are summarized in Table IV. Figs. 8 and 9 indicate that the results obtained from the equivalent circuits are in good agreement with those obtained by conventional FEM. In particular, the equivalent circuit gives the peaks of η accurately although it is generated based on just three snapshots. Once the equivalent circuit is established, η and P can be evaluated much faster than FEM.

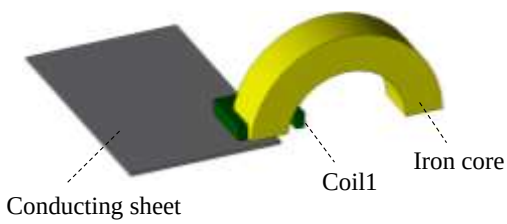

Fig. 7. Models of the induction heating machine

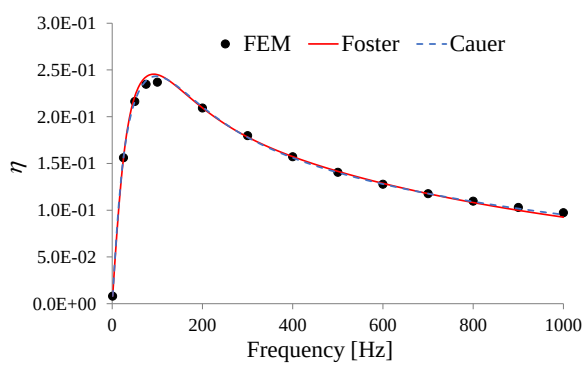

Fig. 8. Frequency characteristic of power factor

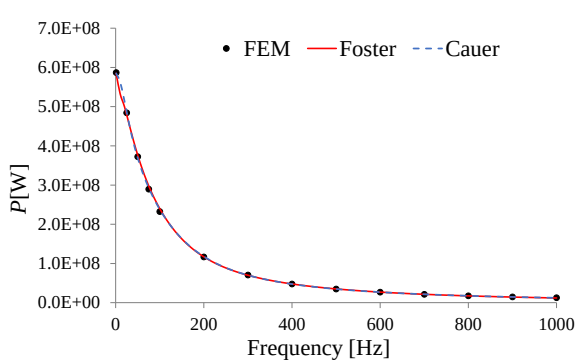

Fig. 9. Frequency characteristic of joule loss

IV. Conclusion

In this paper, we have proposed equivalent-circuit generation from reduced FE models obtained by POD-based MOR. The frequency characteristic of these devices are effectively obtained by solving reduce FE equations whose unknowns are the weighting coefficients to the basis vectors. The circuit parameters of Foster and Cauer circuits are determined from the resultant frequency characteristics using GA. We have applied the proposed method to analysis of the inductor and IH machine under quasi-static approximation. The equivalent circuits derived from the proposed method is shown to give accurate results when sufficient number of ladder stage is used. Once the equivalent circuit is established, we can evaluate various properties such as power factor and loss much faster than the conventional FEM. The extension of the proposed method to nonlinear problems will be future task.

TABLE IV
Circuit parameters

Foster circuit					
N_c	$R_1[\Omega]$	$R_2[\Omega]$	$R_3[\Omega]$	$R_4[\Omega]$	$R_5[\Omega]$
1	1.42×10^{-2}	1.78×10^{-3}	4.59×10^{-7}	2.12×10^{-3}	2.81×10^{-9}
2	2.97×10^{-2}	1.04×10^{-3}	3.20×10^{-3}	2.04×10^{-3}	7.11×10^{-10}
N_c	L_1[H]	L_2[H]	L_3[H]	L_4[H]	L_5[H]
1	4.78×10^{-6}	2.24×10^{-6}	2.10×10^{-5}	7.58×10^{-6}	1.17×10^{-6}
2	4.24×10^{-6}	1.81×10^{-6}	8.63×10^{-6}	1.32×10^{-6}	3.36×10^{-7}
Cauer circuit					
N_c	$R_1[\Omega]$	$R_2[\Omega]$	$R_3[\Omega]$	$R_4[\Omega]$	----
1	4.94×10^{-4}	4.74×10^{-5}	2.41×10^{-4}	1.40×10^{-5}	----
2	1.06×10^{-4}	4.26×10^{-5}	4.33×10^{-3}	3.19×10^{-6}	----
N_c	L_1[H]	L_2[H]	L_3[H]	L_4[H]	L_5[H]
1	5.85×10^{-7}	1.23×10^{-8}	1.34×10^{-9}	2.02×10^{-8}	6.09×10^{-8}
2	2.19×10^{-7}	6.81×10^{-8}	2.48×10^{-9}	3.67×10^{-8}	1.04×10^{-8}

References

[1] B. Gustavsen and A. Semlyen, "Simulation of transmission line transients using vector fitting and modal decomposition," *IEEE Trans. Power Delivery*, vol. 13, no. 2, pp. 60"5-614, April 1998.

[2] K. Yamazaki, "Equivalent Circuit Parameter Calculation of Interior Permanent Magnet Motor Involving Iron Loss Resistance Using Finite Element Method", *IEEJ Trans. IA*, vol. 123, no. 2, pp. 67-74, 2003.

[3] Y. Shindo, O. Noro, "Simple Circuit Simulation Models for Eddy Current in Magnetic Sheets and Wires," *IEEE Trans. Fundamentals and Materials*, vol. 134, no. 4, pp. 173-181, 2014.

[4] P. Feldmann and R. A. Freund, "Efficient linear circuit analysis by Pade approximation via the Lanczos process," *IEEE Trans. Computer-Aided Design*, vol. 14, no. 5, pp. 639-649, 1995.

[5] D. Schmidthausler and M. Clemens, "Low-Order Electroquasistatic Field Simulations Based on Proper Orthogonal Decomposition," *IEEE Trans. Magn.*, vol. 48, no. 2, pp. 567-570, 2012.

[6] A. Odabasioglu, M. Celik, and L. T. Pileggi, "PRIMA: Passive Reduced Order Interconnect Macromodeling Algorithm," *IEEE Trans. Computer Aided Design*, vol. 17, pp. 645-654, 1998.

[7] W. Wang et al., "Fast Frequency Sweep of FEM Models via the Balanced Truncation Proper Orthogonal Decomposition," *IEEE Trans. Antennas Propag.*, vol. 59, no. 11, pp. 4142–4154, Nov. 2011

[8] Y. Sato, F. Campelo and H. igarashi, "Fast Shape Optimization of Antennas Using Model Order Reduction," *IEEE Trans. Magn*, vol. 51, no. 3, 7204304.

[9] Y. Sato and H. Igarashi, "Model Reduction of Three Dimensional Eddy Current Problems Based on the Method of Snapshots," *IEEE Trans. Magn*, vol. 49, no. 5, pp. 1697-1700, May, 2013.

[10] Omar Wing, *Classical Circuit Theory*, Springer, 2010.